Peer-to-Peer Microgrids for 100% Renewable Swarm Electrification: Scalable, Sustainable, Self-Serviceable, Safe, and Stable Design

Hannes Kirchhoff and Kai Strunz

***Abstract*—Swarm microgrids, a specialized type of DC microgrids with peer-to-peer energy exchange, are important enablers for emerging economies seeking climate-friendly and self-sufficient energy access. However, a systematic technology development methodology for swarm microgrids with an explicit long-term expansion perspective is not yet available. To address this gap, this article builds on the existing literature on swarm electrification and presents a structured methodology for the technology design and development of swarm microgrids. The resulting "Quint-S" methodology of five hallmarks is distinguished by a holistic set of three-plus-two governing principles, defined herein. These principles cover the three design features scalability, sustainability, and self-serviceability, as well as the two technical foundations safety and stability. Scalability facilitates the growth from individual solar home systems to swarm microgrids, then to interconnected multi-microgrids, and eventually to interfacing with an AC main grid. Sustainability and self-serviceability ensure that the system uses 100% renewable energy and can be operated by users themselves. The latter characteristic is particularly advantageous in hard-to-reach sites when professional technicians are not available. The results are validated through laboratory experiments and real-world implementation in Bangladesh. The proposed methodology is of interest for a range of applications requiring ad hoc deployment of sustainable infrastructure.**

***Index Terms*—Battery, design methodology, electrical safety, low voltage, microgrid, power electronics, renewable energy, rural areas, stability, sustainable development, swarm electrification.**

NOMENCLATURE

Acronyms

D	Diode.
ELV	Extra-low voltage.
ESMAP	Energy Sector Management Assistance Program.
ICT	Information and communication technology.
ID	Identifier.
IMI	Inter-microgrid interface.
KPR	Key performance requirement.
LAN	Local area network.
MOSFET	Metal-oxide-semiconductor field-effect transistor.
P2P	Peer-to-peer.
PE	Power electronic.
PV	Photovoltaics.
S	Switch.
SBB	Swarm building block.
SELV	Safety extra-low voltage.
SHS	Solar home system.
TVS	Transient voltage suppression.

Subscripts

10	10th.
25	25th.
50	50th.
75	75th.
90	90th.
ACDC	AC–DC converter.
avg	Average.
cap	Capacity.
DCDC	DC–DC converter.
IMI	Inter-microgrid interface.
line	Line.
link	Link.
max	Maximum.
n	Node, nodal.
PE	Power electronic.
ref	Reference.
s	Supply.

Variables and Operators

E	Energy.
F	Factor.
i, I	Current.
j	Swarm unit index.
k	Line index.
P	Power.
q	Percentile.
R	Resistance.
T	Time period.

Manuscript received 24 April 2023; revised 30 September 2023; accepted 24 January 2024. Date of publication 8 February 2024; date of current version 18 April 2024. This work was supported by a Ph.D. scholarship from the Hans-Böckler Foundation, co-funded by the Federal Ministry of Education and Research (Germany). *(Corresponding author: Hannes Kirchhoff.)*

Hannes Kirchhoff is with the Chair of Sustainable Electric Networks and Sources of Energy (SENSE), Department of Energy and Automation Technology, Technische Universität Berlin, 10587 Berlin, Germany, also with the ME SOLshare, Dhaka 1229, Bangladesh, and also with the ME SOLshare, Singapore 068808 (e-mail: microenergy.kirchhoff@gmail.com).

Kai Strunz is with the Chair of Sustainable Electric Networks and Sources of Energy (SENSE), Department of Energy and Automation Technology, Technische Universität Berlin, 10587 Berlin, Germany (e-mail: kai.strunz@tu-berlin.de).

Color versions of one or more figures in this article are available at https://doi.org/10.1109/JESTIE.2024.3363667.

Digital Object Identifier 10.1109/JESTIE.2024.3363667

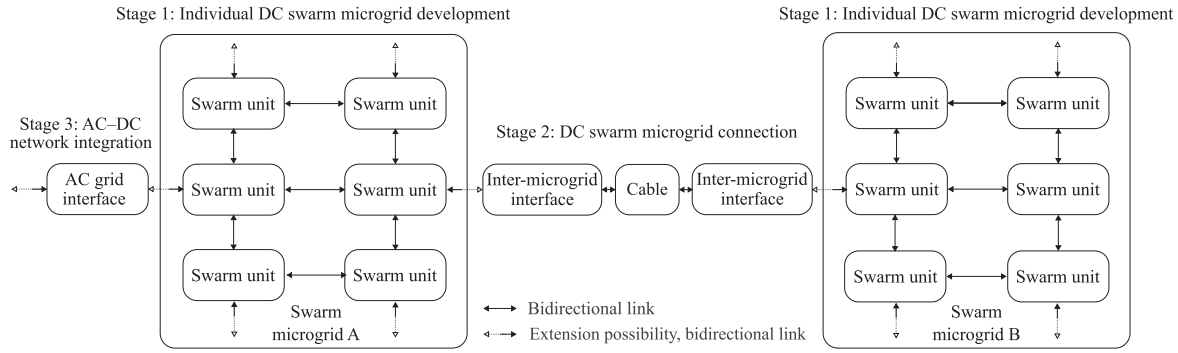

Fig. 1. Swarm electrification concept: Individual DC swarm microgrid development in Stage 1; DC swarm microgrid connection in Stage 2 using inter-microgrid interfaces (IMIs); AC–DC network integration in Stage 3.

t	Time.
v, V	Voltage.
Δ	Difference operator.
η	Efficiency.

I. Introduction

GLOBALLY, 675 million people still lack access to electricity [1]. Swarm electrification is intended to address this situation by enhancing access to electricity through a transition from standalone solutions to microgrids with peer-to-peer energy exchange [2].

Swarm electrification is based on the so-called swarm microgrid [3], which is a specialized type of DC microgrid. The development of DC microgrids has made considerable progress over the past decade [4], [5]. By using DC instead of AC, the energy losses of a microgrid can be reduced by up to 50% [6].

Swarm electrification is defined as an electrification development process that encompasses multiple stages. The three main stages are shown in Fig. 1 and explained as follows. In Stage 1, DC swarm microgrids are developed individually, enabling peer-to-peer (P2P) energy exchange between so-called swarm units. These swarm units are houses and business units that already have existing standalone energy systems. The standalone systems considered in this work are solar home systems (SHSs), of which six million have been installed in Bangladesh alone [7]. In Stage 2, the swarm microgrid as a whole is interconnected to neighboring swarm microgrids. In Stage 3, as a possible but not necessary step, the integration with an AC main grid may allow for energy purchases from the outside. A prerequisite for this last stage is, of course, the eventual availability of the main grid close to the DC swarm microgrid.

Swarm electrification has received considerable recognition as an innovative solution for addressing the parallel challenges of climate change mitigation and access to electricity [8]. For access to electricity applications, demand typically grows in a pattern of multiple tiers [9], [10]. To cater to this stepwise demand development, swarm electrification is centered around the principle of organic growth, allowing infrastructure to grow with demand and thereby avoiding oversizing and saving costs. Along the infrastructure growth path, the expansion steps are incremental. Each incremental expansion step is associated with comparatively low costs, contributing to the affordability of swarm microgrids [2], [11].

While the conceptual and economic literature on swarm electrification is extensive, the literature on the technology for swarm electrification is scarce. A recent review paper on swarm electrification emphasized the lack of technical definitions for swarm microgrids [12]. In what follows, this shortcoming is addressed by the presentation of a holistic design methodology for swarm microgrids. The presented methodology significantly extends the existing knowledge on microgrid planning [13], [14] and directly supports previously identified key drivers of swarm microgrid development [15]. Three of these previously identified key drivers are directly related to the technology design, concerning extendability, ease of use, and quality of service [15]. Accordingly, these three factors need to be addressed by the technology design methodology and are discussed as follows.

Extendability has recently been recognized as a key promise of DC microgrids, especially in the context of energy access applications [16]. To achieve extendability, various configurations have been proposed. These configurations fall into the following three categories. The first category comprises microgrids with centralized storage and centralized generation [14], [17]. The second category consists of microgrids with mainly centralized generation but decentralized storage [16], [18]. The third category, which includes swarm microgrids, corresponds to configurations with both decentralized generation and decentralized storage [19], [20]. In addition to individual microgrids, multi-microgrid topologies with interconnections between microgrids have also been discussed [21], [22]. However, the literature still lacks details on the development paths that allow for transitions from one topology to another. More specifically, there is currently no methodology that encompasses the development and extension prospects of swarm microgrids to ensure readiness for future expansion steps.

Ease of use requires a technology that adheres to a range of requirements [15], [23]. As minimum criteria, the technology must be robust and safe to use [12]. Regarding robustness, factors that cause instability have been identified [24], [25] and suitable mitigation strategies validated [3], [26], [27]. Concerning the deployment of safe-to-use technology at hard-to-reach

sites, various low-voltage DC microgrid solutions have been discussed [28], [29]. These solutions differ in terms of grounding and the degree of system reliability achieved through zonal protection [30], [31], [32]. For applications in the energy access context, extra-low voltage (ELV) systems have been proposed [16], [33] with voltage levels that are safe to touch [34], [35]. However, the literature still lacks a safety design methodology for swarm microgrids that users are able to easily operate and maintain by themselves.

Quality of service is related to the reliability of power and requires a suitable power supply strategy [15]. Power generation should rely only on renewable energy technologies. However, these power sources have variable output. Therefore, the microgrid needs to integrate storage capacity [4], [36]. One core attribute of swarm electrification is the integration of the SHSs' generation and storage capacity into the swarm microgrid [2]. Initial practical validations of the integration of the generation and storage capacity of SHSs into DC microgrids have been evaluated in the literature [33], [37]. These validations have been limited in that the number of participating units has been fewer than ten [37] or in that they have focused on a theoretical assessment of how to reach the full sharing potential [33]. However, the literature still lacks an assessment of practical large-scale implementation of renewable-energy-powered swarm microgrids, in particular in regards to the quality of service provided.

This article addresses the highlighted gaps in the literature by making the following two key contributions: first, the presentation of the so-called "Quint-S" methodology, a fully integrated microgrid design methodology for swarm electrification; second, the validation of this methodology, by means of laboratory experiments as well as large-scale field implementation of a scalable, sustainable, self-serviceable, safe, and stable microgrid solution for the electrification of remote locations in the Global South.

The proposed methodology is defined by three-plus-two governing principles, categorized into two sets. The first set specifies the design features of scalability, sustainability, and self-serviceability. The combination of these design features offers a structured and staged swarm electrification that supports climate goals and allows for users to perform operations and installations, even if professional assistance is unavailable. The second set covers the technical foundations of safety and stability, which cannot be compromised and serve as constraints to be respected while striving to meet the objectives defined by the design features.

Overall, this article introduces and describes the first comprehensive technical methodology for designing DC microgrids using modular building blocks that lend themselves to bottom-up swarm electrification in the Global South. At the heart of this novel framework is the rigorous enforcement of the newly proposed "Quint-S" methodology, which enables technical system integration thanks to the five presented hallmarks of scalability, sustainability, self-serviceability, safety, and stability. Without neglecting the holistic perspective, this article focuses on how the inclusion of renewable sources and power hardware, protection, and information and communication technology is essential for achieving sustainability, safety, and self-serviceability at widely different scales of propagation. The pioneering claims made are validated by laboratory experiments, real-world field implementation, and true operating experience in Bangladesh. The successful implementations in Bangladesh are universally achieved at 100% renewable energy, thus meeting standards of far-reaching climate objectives already today.

The rest of this article is organized as follows. Key performance requirements (KPRs) for all three stages of swarm electrification are discussed in Section II. The design features of scalability, sustainability, and self-serviceability are introduced in Section III. The design foundations of safety and stability are discussed in Section IV. The implementation process flow for the proposed methodology is provided in Section V. Validations, including the real-world application of the proposed microgrid design methodology in Bangladesh, are presented in Section VI. Conclusions are drawn in Section VII.

II. Key Performance Requirements

In this section, KPRs and associated specifications are derived for all stages of the swarm electrification pathway, which is laid out in Section I and illustrated in Fig. 1. These KPRs form the basis for and serve as specifications of the designs presented in the subsequent sections. A summary of the KPRs is provided in Table I. For each stage, the KPRs cover system-wide specifications as well as related and distinct specifications for interfaces and interlinks.

A. Stage 1: Individual DC Swarm Microgrid Development

As shown in Fig. 1, a DC swarm microgrid consists of swarm units and bidirectional links between these swarm units. On this basis, the DC swarm microgrid must support P2P energy exchange between the swarm units. Swarm microgrids are expected to be used in geographical locations where dedicated service personnel are not readily available. Therefore, the technology has to be modular, transportable, and be able to be carried, installed, and operated by the users themselves. No dedicated service personnel should be needed.

In accordance with the overarching system specifications, the requirements set for the interface of a swarm unit are threefold. First, the technology is to integrate with the existing energy assets. These existing resources are SHSs, each one consisting of solar photovoltaics (PV), batteries, and loads. Second, the interface of the swarm unit is to enable bidirectional power flows between an SHS and other swarm units. Third, the technology is to facilitate meshed network configurations. A so-called swarm building block (SBB), as defined in Fig. 2 of Section III, is implemented to realize these interface specifications.

For Stage 1, interlinks are specified as follows. The energy to be supplied by an interlink needs to cater to a swarm unit drawing 200 Wh per day, denoted as a nodal energy exchange of $|E_{\mathrm{n}}| = 200$ Wh per day. The value of 200 Wh per day is derived from the load requirements as per the World Bank's ESMAP energy access level two [9]. A minimum distance of 100 m is to be bridged.

TABLE I
KPRs OF SWARM ELECTRIFICATION

Stage	KPR I Stage 1: Individual DC swarm microgrid development	KPR II Stage 2: DC swarm microgrid connection	KPR III Stage 3: AC–DC network integration
System specification	Allows for P2P energy exchange between swarm units in a meshed DC microgrid using a modular, transportable, and highly cost-effective technology that can be installed and operated by untrained users.	Provides energy balancing between two swarm microgrids via a DC link using a connection technology that is installed and operated by trained users.	Adapts the swarm microgrid to the role of an active resource as seen from the AC main grid using a connection technology that is installed by qualified technicians, but operated by trained users.
Interface specification	Swarm building block (SBB): Integrates with the existing energy assets. Provides the ability to form meshed network configurations of the swarm microgrid. Enables power flows between an SHS and other swarm units.	Inter-microgrid interface (IMI): Integrates with a swarm microgrid. Provides the ability to form a point-to-point connection with another swarm microgrid. Enables power flows between two swarm microgrids.	AC grid interface: Integrates with a swarm microgrid. Provides the ability to use the swarm microgrid as an active resource to the AC grid. Enables power flows between the AC main grid and the swarm microgrid.
Interlink specification	Enables the transfer to cater to nodal energy exchange of $\lvert E_{\mathrm{n}}\rvert = 200$ Wh per day. Distances of up to 100 m must be covered.	Enables the transfer to cater to $E_{\mathrm{IMI}} = 1000$ Wh per day. Distances of up to 1000 m must be covered.	Enables the transfer of at least $E_{\mathrm{ACDC}} = 8400$ Wh per day. The AC main grid connection is in direct proximity to the swarm microgrid.

As for the following stages, a voltage drop of no more than 10% must be maintained. To limit the cost of cabling and reduce the risk of cable theft, cables with a cross section of 2.5 mm^2 are used. Wherever required, DC–DC converter efficiency is approximated with $\eta_{\text{DC-DC}} = 0.98$ [38].

B. Stage 2: DC Swarm Microgrid Connection

As shown in Fig. 1, the DC swarm microgrid connection is an extension of Stage 1. The DC swarm microgrid connection is specified to support energy balancing between two swarm microgrids. The connection consists of two inter-microgrid interfaces (IMIs) and a cable between them. The installation requirements are similar to those of Stage 1, but now users performing the installation are assumed to have received basic training. As provided in Table I, the interface specifications now extend to the microgrid connection. Accordingly, links need to cover longer distances and daily energy demands according to the World Bank's ESMAP energy access level three [9].

C. Stage 3: AC–DC Network Integration

As shown in Fig. 1, the AC–DC network integration is a further possibility for extension. The main objective in this stage is to change the role of a swarm microgrid to that of an active resource from the perspective of the AC main grid. The installation requirements are different from those in the previous stages because qualified technicians are required to establish the connection to the AC main grid. Extended interface specifications address the potential connection to the AC grid, as described in Table I. Interlinks need to cater to the World Bank's ESMAP energy access level five [9].

III. Design Features for Scalability, Sustainability, and Self-Serviceability

The KPRs of Table I can be met by the integrated set of design features of scalability, sustainability, and self-serviceability. This set of design features accompanies the entire multistage swarm electrification process depicted in Fig. 1. As follows, the three design features are discussed in reverse order.

Self-serviceability refers to the ability of users to perform the actions required to ensure continuous operation without depending on service personnel. This design feature is particularly important considering that swarm microgrids may be located in hard-to-reach sites and may also be used by mobile populations who regularly move to different locations. The infrastructure needs to be deployable and serviceable by the users themselves.

Self-serviceability must be supported through a power and control layer and an information and communication technology (ICT) layer. The power and control layer facilitates the required power flows in the bidirectional links shown in Fig. 1 The ICT layer ensures that the digital systems within a swarm microgrid can facilitate P2P energy sharing and enforce the respective business models. While the swarm microgrid must be self-serviceable onsite, a remotely located organization can support the community through the ICT infrastructure, too.

As core requirements, the ICT infrastructure needs to provide remote monitoring and remote troubleshooting capabilities. In addition, billing capabilities are required for the P2P energy exchange in Stage 1. Remote monitoring refers to the ability to assess the performance of the swarm microgrid and its integration with other networks remotely. Remote troubleshooting refers to the ability of the support organization to provide real-time updates to the provisioned technology and guide users interacting with the hardware on-site. Billing in energy access applications is commonly implemented with a prepaid billing scheme. As such, the ICT infrastructure needs to provide capabilities for top-up and cash-out of the individual SBBs' prepaid balances.

While the requirements in terms of self-serviceability are mandatory in Stage 1, a high level of self-serviceability is still very desirable in Stages 2 and 3. The corresponding provisions to attain self-serviceability are integrated with the following two "S" design features and the two "S" technical foundations presented in Section IV.

Sustainability of swarm electrification is addressed by ensuring that the generation portfolio relies only on renewable energies. This is essential to support climate change mitigation and

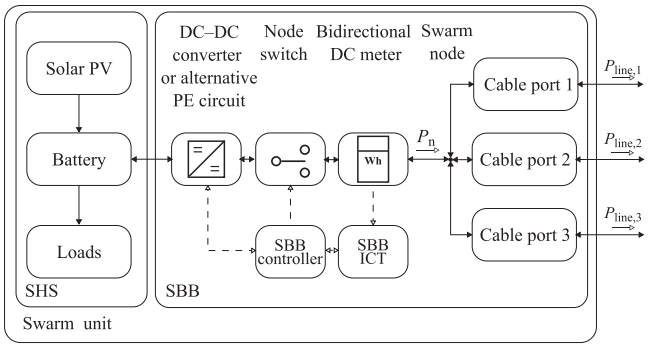

Fig. 2. Detailed modular architecture design for a swarm unit, including the existing solar home system (SHS) and the swarm building block (SBB) with power electronic (PE) circuit.

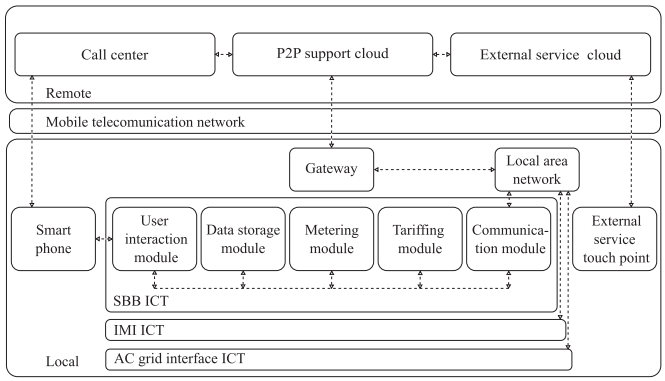

Fig. 3. Architecture of the ICT layer, including local and remote ICT facilities.

to minimize the local fuel import dependency of communities using swarm microgrids.

The remainder of this section focuses on scalability. To realize scalability, modular architectures are used to support the stagewise advancement of swarm electrification. The realization of the specification of the daily energy transfer capacity takes advantage of the availability of distributed storage and goes beyond the mere consideration of constraints set by the carrying capability of the lines. In the following, the modular architecture and storage–line–storage interlinks are elaborated for all three stages.

A. Stage 1: Individual DC Swarm Microgrid Development

As early as in the first stage, the DC swarm microgrid development itself is modular and uses storage–line–storage interlinks to attain scalability. It so supports KPR I of Table I.

1) Modular Architecture of the Power and Control Layer: As shown in Fig. 1, the swarm microgrid architecture consists of connected swarm units. To ensure that the swarm microgrid becomes modular and even transportable, the presented design makes use of distributed SBBs, as depicted in Fig. 2. An SBB is installed at every swarm unit of the microgrid.

As shown in Table I, a swarm unit adopts multiple roles. It integrates with existing energy assets, it enables bidirectional power flows between the SHS and other swarm units, and it provides the ability to form a meshed network configuration. To ensure integration with existing energy assets of the SHS, each SBB directly interfaces with the battery of the SHS, as shown in Fig. 2.

To enable bidirectional power flows to and from the SHS, the SBB includes five components between the SBB's swarm node and the SHS battery, as depicted in Fig. 2. First, a bidirectional meter is required for billing. Second, this meter interfaces the SBB ICT modules shown in Fig. 3. Third, a nodal switch is required to enable or disable power flows between the SHS and the SBB. Fourth, a DC–DC converter may be used to control the node voltage independently of the battery voltage. Instead of the DC–DC converter, alternative power electronic (PE) circuits can be used. As a minimum requirement, such a circuit needs to provide the capability to control the direction of the power flow. Details of such alternative circuits are discussed in Appendix D. Fifth, the three last-mentioned components are connected to the SBB controller, which enables automated operation of an SBB.

The SBB's cable ports serve as the connection points for interconnections with other swarm units. As depicted in Fig. 2, these cable ports are joined at the swarm node. Each line in the microgrid is connected between two SBBs via cable ports. Ring network configurations can be established with two cable ports per SBB. Meshed network configurations require more than two cable ports per SBB.

2) Modular Architecture of the ICT Layer: The minimum requirements for the ICT layer, as defined in the introduction of Section III, are remote monitoring, remote troubleshooting, and balance-update facilities for prepaid billing. To address the requirements, a fundamental ICT architecture, as shown in Fig. 3, is derived as follows. The architecture facilitates management of the P2P energy exchange by a support organization and spans both local and remote ICT facilities.

Locally, most ICT facilities reside within the SBBs. Each SBB needs to incorporate the following five modules, as shown in the bottom section of Fig. 3. First, a user interface module permits visualization of the prepaid metering balance and enables user interaction with the SBB. Second, a data storage module acts as a data buffer prior to data upload to the cloud for remote monitoring and remote troubleshooting. Third, a metering module digitizes quantities of energy exchanged as measured by the bidirectional DC meter depicted in Fig. 2. Fourth, a tariffing module applies the prevailing tariff on a particular exchanged energy quantity and updates the balance of the SBB. The tariffing module also includes a local ledger that records exchanged energy quantities. Fifth, a communication module provides a connection to a local area network (LAN) connection. This LAN can also be utilized by local ICT facilities of later stages, namely the IMI ICT for Stage 2 and the AC grid interface ICT for Stage 3. The LAN is connected to the cloud through a gateway with the mobile telecommunication network.

With the five modules of the SBB ICT, P2P energy exchange can be undertaken anytime, even if the connection to remote ICT facilities is temporarily unavailable. When exchanging energy with other swarm units, the SBB updates the balance in real time, applying the prevailing tariff. In parallel, the SBB records

data for later monitoring activities. This data is then sent to the remote ICT facilities when a connection is available. Relevant data record standardization formats, specifically designed for scenarios with high volatility in the availability of the mobile telecommunication network, are discussed in [39]. Data monitoring and changes to the P2P energy exchange tariff scheme are undertaken centrally by means of the remote ICT facilities.

Remote ICT facilities include three core services. First, the support organization's call center interacts with users to provide data-backed remote troubleshooting. Second, the P2P support cloud is the central point of device communication with all SBBs, enabling remote monitoring as well as updates to tariff schemes and device configurations. Third, external service providers are included in the ICT infrastructure. For example, mobile money service providers typically have local vendors, which are integrated into the ICT infrastructure for seamless top-up and cash-out services.

3) Storage–Line–Storage Interlinks: The maximum power $P_{\text{line,max}}$ transferable over a line connecting two swarm units in a swarm microgrid of Fig. 1 is constrained by the supply voltage V_{s}, the maximum voltage drop ΔV_{max} along the line, and the line resistance R_{line} as follows:

$$P_{\text{line,max}} = (V_{\text{s}} - \Delta V_{\text{max}}) \cdot \frac{\Delta V_{\text{max}}}{R_{\text{line}}} . \tag{1}$$

Disregarding the storage at sending and receiving swarm units and considering that both power generation from PV and load power are generally intermittent, the power flow on the line is also intermittent. The intermittency also influences the energy E_{line} that is transferred over the line. This energy may be expressed by $P_{\text{line,max}}$ multiplied by T_{line} as follows:

$$E_{\text{line}} = P_{\text{line,max}} \cdot T_{\text{line}} , \tag{2}$$

where T_{line} denotes the time interval during which the line would need to be operated at maximum power to yield E_{line}. For a reference period T_{ref}, with $T_{\text{line}} \leq T_{\text{ref}}$, the interval T_{line} can be related to a capacity factor $F_{\text{cap,line}}$ [40] as follows:

$$F_{\text{cap,line}} = \frac{T_{\text{line}}}{T_{\text{ref}}} . \tag{3}$$

Combining (2) and (3) yields

$$E_{\text{line}} = P_{\text{line,max}} \cdot F_{\text{cap,line}} \cdot T_{\text{ref}} . \tag{4}$$

However, in terms of the coordination of the energy transfer between swarm units, the battery, as a key component of the swarm unit, is important, too. With storage being present on both ends of the line, an interlink can be regarded as a storage–line–storage subsystem. Because of this storage, the concurrent availability of both nodes for sending and receiving power flows on the line is increased. The capacity factor thus increases to $F_{\text{cap,link}} \geq F_{\text{cap,line}}$. Therefore, the energy transfer capacity E_{link} for such an interlink is formulated as

$$E_{\text{link}} = P_{\text{line,max}} \cdot F_{\text{cap,link}} \cdot T_{\text{ref}} . \tag{5}$$

An important factor that influences the capacity factor $F_{\text{cap,link}}$ is the storage size available to facilitate load leveling [41]. For the SHS in a swarm microgrid, the storage capacity is a multiple of the daily load requirement [42]. Against this background, high values of $F_{\text{cap,link}}$, up to $F_{\text{cap,link}} = 1$, are feasible.

TABLE II
ENERGY TRANSFER CAPACITY OVER $T_{\text{REF}} = 24$ H WITH $k \in \{1, 2, 3\}$

V_{s} [V]	$P_{\text{line,max},k}$ [W]	$E_{\text{link},k}$ [Wh]	$\lvert E_{\text{n,max}} \rvert$ [Wh]
12	8.7	209	627
24	34.9	837	2 511
48	139.6	3 350	10 050

V_{s}: Voltage at the swarm node of the supplying swarm unit.
$F_{\text{cap,link}} = 1$, 2.5 mm^2 cross section, 100 m length, 10% voltage drop.

With $T_{\text{ref}} = 24$ h, the resulting daily energy transfer capacity $E_{\text{link},k}$ of an interlink k in a swarm microgrid is provided in Table II. In addition, the total nodal energy transfer capacity $|E_{\text{n,max}}|$, when using all three interlinks $k \in \{1, 2, 3\}$ of a swarm unit, is given. The energy transfer requirement for Stage 1 of 200 Wh per day, as formulated in Section II and presented in Table I, is met even at a very low supply voltage such as 12 V.

B. Stage 2: DC Swarm Microgrid Connection

In the second stage, the DC swarm microgrid connection of two swarm microgrids is realized to support KPR II of Table I. As depicted in Fig. 1, a DC swarm microgrid connection facilitates energy transfer between two swarm microgrids by using two IMIs and a cable between them. This energy transfer occurs at higher voltage levels compared with those applied within the swarm microgrids. Details on the modular architecture for Stage 2 are provided in Appendix A.

As also shown in Fig. 1, an IMI-connected swarm unit has three links to transfer energy to other swarm units of the same microgrid. To transfer the required 1000 Wh per day, as specified in Table I, each of the three links must be able to transfer at least 340 Wh per day. This corresponds to $1000/3$ Wh plus a margin to cover the conversion losses within the SBB. As shown in Table II, this can be accomplished when the supply voltage selected for the swarm microgrid is at least 24 V.

C. Stage 3: AC–DC Network Integration

The connection of the AC grid to a swarm microgrid may be realized in a third stage, fulfilling KPR III of Table I. The AC grid interface of Fig. 1 enables power flows between the AC grid and the connected swarm microgrid. Details on the modular architecture for Stage 3 are discussed in Appendix B.

To transfer the required 8400 Wh per day, as mandated in Table I, all of the other three available links originating from the swarm unit connected to the AC grid interface in Fig. 1 must be able to transfer at least 2800 Wh per day. As shown in Table II, this can be accomplished when the supply voltage selected for the swarm microgrid is at least 48 V.

IV. DESIGN FOUNDATIONS FOR SAFETY AND STABILITY

Building on the design features in Section III, the design foundations of safety and stability for all three stages of swarm electrification are presented in this section. Stability is a key requirement for the operation of microgrids in general. To achieve

TABLE III
DETAILED PROVISIONS TO ENSURE SAFETY IN ALL THREE STAGES OF SWARM ELECTRIFICATION AND RELEVANT STANDARDS

Verification category	Individual DC swarm microgrid development	DC swarm microgrid connection	AC–DC network integration	Relevant standards
Protection against electric shock	Basic protection through insulation. Fault protection by using safety extra-low voltage (SELV). The system therefore does not need to be grounded, and all voltages must be below 120 V.	Basic protection through insulation. Fault protection through double insulation. Cables and DC–DC converters must have double insulation. Converters must have galvanic separation with double or reinforced insulation to prevent dangerous voltages on the SELV side.	Basic protection through insulation. Fault protection on the AC side in compliance with local regulations. The AC–DC converter must have galvanic separation with double or reinforced insulation to prevent dangerous voltages on the SELV side.	IEC 60364-4-41, IEC 62477-1, IEC 60335-1, IEC 60335-2, IEC 61558-2-16
Protection against thermal effects	Placement of a fuse in each cable port to prevent cable overheating. Overtemperature protection for any DC–DC converter, if used.	Provisions in the design and control of the DC–DC converters to address cable and DC–DC converter overheating.	Provisions in the design and control of the AC–DC converters to address cable and AC–DC converter overheating.	IEC 60364-5-42, IEC 60950-1, IEC 61204
	The charging parameters of the SHS batteries must be respected to prevent battery overheating and gassing.			IEC 62093, IEC 62509, EN 50272-2
Protection against overcurrents and short circuits	Coordination of the tripping of the abovementioned fuses in each cable port using a zonal protection scheme.	Limiting of the maximum current in the cables in accordance with the DC–DC converter capacity.	Limiting of the maximum current in the cables in accordance with the AC–DC converter capacity.	IEC 60464-4-43, DIN VDE 0298-4, IEC 62477-1, IEC 62485-1
Protection against disturbances	Warning signs indicate that maintenance work must not be performed during lightning events. Surge protection for lightning-induced surges provided in the SBB at the node bus.	Burial of the DC cable to reduce the likelihood of lightning flashes to lines. Surge protection for lightning-induced surges provided in each inter-microgrid interface between the cable and the dc meter.	Compliance with local regulations. Surge protection on AC side by ability to withstand voltages of at least 2.5 kV, or as per local regulations.	IEC 60364-4-44, IEC 61000-6-1
	Further lightning protection must be provided in compliance with findings of a site-specific assessment. Compliance with relevant standards concerning electromagnetic compatibility (EMC) must be ensured.			IEC 62305-2, IEC 62561-2, EN 55022, EN 55014-1, EN 55014-2
Safe separation	Provision of the ability to safely disconnect batteries.			
	No further requirements for safe separation, as SELV is used.	Supply disconnection for both IMIs via electromechanical relays if the line is interrupted.	Provision of a circuit breaker or switch to disconnect the AC supply.	IEC 60364-4-46, IEC 60950-1, IEC 62477-1

stability in the context of swarm electrification, decentralized and robust control schemes are of interest. Control schemes that address such aspects are described in the literature [3], [4], [43]. Therefore, this section focuses on safety, the second design foundation.

The safety design process encompasses the following steps:

(a) Evaluation of the unique needs arising in the swarm electrification context. As detailed in Table I, the needs that arise in the swarm electrification context are unique because the operation and maintenance of swarm microgrids cannot depend on dedicated service personnel due to the often-remote locations of the installation sites. Furthermore, a swarm microgrid is a transportable infrastructure that can be expanded and relocated quickly.

(b) Specification and development of main protective measures of the safety design to address the identified needs: The following three main guiding principles for protective measures to ensure microgrid safety are proposed in accordance with the identified needs. First, every part of the infrastructure accessible during usage is implemented as a safety extra-low-voltage (SELV) system [34]. Second, for integrating supply from networks with voltage above the extra-low voltage, the design makes use of power conversion technology with double or reinforced insulation and built-in safety provisions [34]. Third, the technology is highly modular and utilizes zonal protection to isolate faults.

(c) Verification of the key provisions made to fulfill requirements in accordance with relevant safety standards: Beyond being tailored to the particular requirements of swarm electrification, it is important that the safety design also complies with given standards. For verification, relevant requirements are derived from the IEC 60364 and VDE 0100 standard series.

An overview of complete set of relevant standards and detailed provisions undertaken for all stages are provided in Table III. In the following, the key safety provisions for all stages are discussed.

A. *Stage 1: Individual DC Swarm Microgrid Development*

In the first stage, the DC swarm microgrid development KPR I of Table I is to be fulfilled. The first key need to be addressed is the mitigation of the considerable risk of electric shock, as the technology must be usable and serviceable even by untrained users. Conventionally, the most common method for protection

against electric shock is to use insulation as basic protection and automatic disconnection of the supply as fault protection. However, such automatic disconnection of the supply requires grounding [34] and continuous quality monitoring of the grounding system [35]. Because the system must be installable and serviceable by users, protection measures that require such continuous quality monitoring of a grounding system are not applicable here. For this reason, the main protective measure of using SELV as the system voltage is applied here to ensure safety, as discussed under item (b) above. An installation with SELV does not require grounding.

The second key need is to avoid the spread of short-circuit faults through the network. Due to the meshed network configuration of the swarm microgrid, such faults could quickly spread through a large portion of the network. To address this need, the main protective measure of applying zonal protection, as described under item (b) above, is utilized. The cable ports of each SBB, as shown in Fig. 2, are equipped with individual cable overcurrent protection devices, such as fuses. With this measure, faults are isolated before they can spread to other parts of the network.

B. Stage 2: DC Swarm Microgrid Connection

In the second stage, the DC swarm microgrid connection, the KPR II of Table I is addressed. The first key need in this stage is to achieve longer transfer distances without compromising safety. This need is addressed by following the guiding principle of using conversion technology with double or reinforced insulation, as described under item (b) above. Such insulation allows for the cable between two IMIs to be operated at a voltage higher than SELV while maintaining safety for users in the swarm microgrids, which are implemented with SELV. The DC swarm microgrid connection does not contain any loads, but instead consists only of two IMIs and a cable between them, all of which can be secured with double or reinforced insulation.

The second key need is to avoid the spread of fault currents. Again, a zonal protection scheme is used, as mentioned under (b) above. Accordingly, the power electronic converter's built-in overcurrent protection is used to prevent the spread of fault currents from the DC swarm microgrid connection to the swarm microgrid or vice versa.

C. Stage 3: AC–DC Network Integration

The third stage, AC–DC network integration, is aimed at fulfilling KPR III of Table I. To ensure safety in this stage, the potentially dangerous AC supply must be separated from the SELV system that users can access. Therefore, the first key need for the integration of the AC grid with the swarm microgrid is the safe conversion between AC power and SELV DC power. This need is addressed with the main protective measure of using conversion technology with double or reinforced insulation, as described under item (b) above. Accordingly, double or reinforced insulation is a mandatory requirement for the AC–DC converter.

The second key need that must be met in this stage is to avoid the spread of fault currents. This is accomplished by means of a zonal protection scheme, as described under item (b) above, in which the power electronic converter's built-in overcurrent protection is used to prevent the spread of fault currents from the AC grid to the swarm microgrid or vice versa.

V. Flowchart of the "Quint-S" Methodology

While the "Quint-S" methodology is holistic thanks to its five "S" governing principles for design and technical foundation, its successful application also relies on an orderly implementation through a structured process. For this purpose, a process flowchart was developed to support swarm electrification based on the "Quint-S" methodology. It is different from typical linear processes of microgrid realization where a microgrid planning stage is followed by an implementation stage. Instead, the realization process for swarm microgrids is iterative with incremental changes undertaken after deployment. Thus, before a first deployment and thereafter, aspects of design and technical foundations are covered throughout swarm microgrid development. The process flowchart for swarm microgrid deployment is provided in Fig. 4. The flowchart is structured, from left to right, along the five governing principles of the developed methodology. The flowchart is decomposed into three parts, each covering one stage and described as follows.

A. Stage 1: Individual DC Swarm Microgrid Development

Typically, there are already individual standalone energy systems in the form of SHSs available at the start of Stage 1. Each of these SHSs has battery storage and solar PV. As demand grows, a swarm microgrid becomes an attractive alternative to standalone solutions. The SHS users and other members of the community then jointly agree on the requirements for the swarm microgrid development; the definition of KPR I of Table I acts as a guideline. Based on the required energy transfer demand E_{n}, the microgrid supply voltage V_{S} is selected as per Table II. The SBBs are implemented following the architecture depicted in Fig. 2, including the ICT facilities of Fig. 3. If this is the initial deployment of SBBs or if a change in the SBB design requires an update of the installed SBBs, the technical foundations of stability and safety need to be addressed before deployment.

Stability requires a control scheme that makes use of the decentralized storage capacity integrated into the swarm microgrid. Such a control scheme was described and validated in [3]. The control parameters are selected to ensure robustness across a wide operating envelope. In addition, stability is proven in a laboratory environment prior to deployment.

Safety is addressed by the measures discussed in Section IV. For the SBBs in Stage 1, this requires SELV to be used and zonal protection to be implemented by respective overcurrent protection devices in the cable ports of the SBB. All safety provisions provided in Table III are undertaken prior to deployment.

Following the self-serviceability principle, the SBBs can now be installed by users themselves. The deployed ICT infrastructure allows for remote monitoring and provides a means to guide the community regarding future extensions.

The microgrid is scaled by adding further swarm units and can also include the integration of other grids. Should the community

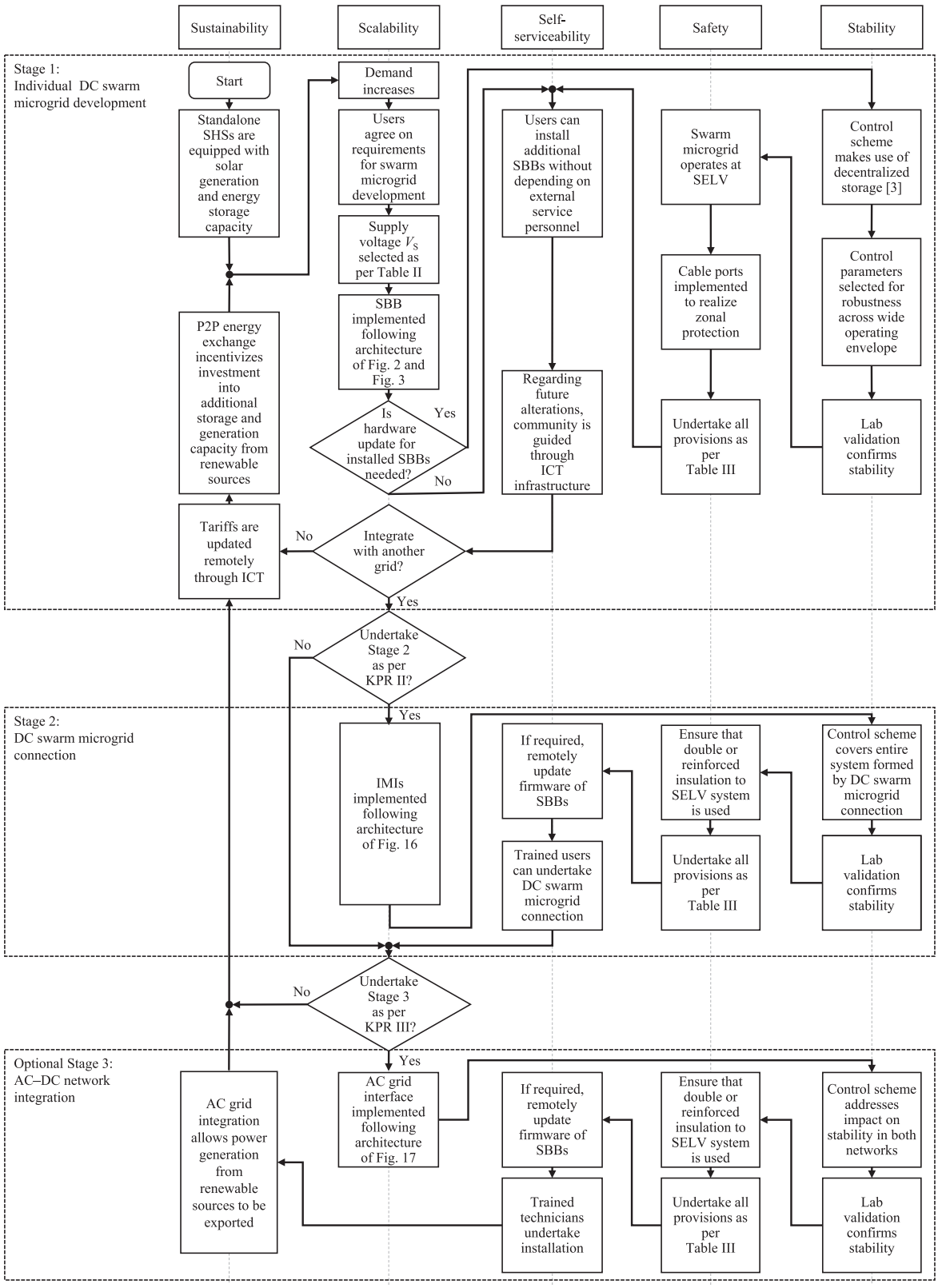

Fig. 4. Implementation process flow of the "Quint-S" technology design methodology for swarm microgrids.

decide to undertake such integration, the process continues with Stage 2. Otherwise, the process stays within Stage 1, and the next step falls under the governing principle of sustainability.

The tariffs for the P2P energy exchange are changed remotely whenever incentives need to be changed. The tariff scheme is set to encourage investments in electricity generation capacity from renewable sources. In addition, the intermittency of renewable energies is addressed by having sufficient energy storage capacity available in the swarm microgrid. Therefore, respective investments into storage capacity are incentivized. Details on a tariff scheme design that supports investments while respecting sustainability criteria were discussed in [15].

B. Stage 2: DC Swarm Microgrid Connection

With regard to further scaling of the infrastructure, the community may decide to undertake a DC swarm microgrid connection that fulfills KPR II of Table I. The IMIs are implemented in accordance with the architecture provided in Fig. 16.

The control scheme for this Stage 2 must ensure stability for the entire system, spanning across the two connected swarm microgrids. To this end, the control scheme design can make use of the storage capacity directly connected to an IMI, as shown in Fig. 16. Laboratory validation then confirms the stability of the control scheme.

To ensure safety, double or reinforced insulation needs to be used to prevent dangerous voltages on the SELV side. All safety provisions as per Table III must be provided.

Self-serviceability is supported via ICT in that remote updates of the SBBs already installed can be undertaken. For example, this support can be used to update reference parameters of the power electronic circuit of the SBB. The installation of the DC swarm microgrid connection can be undertaken by trained users.

After Stage 2 deployment, the community is asked whether the swarm microgrid should be connected to an AC grid if there is one available in the vicinity. If the community wants such a connection to the AC grid that fulfills KPR III of Table I, the process continues with Stage 3; otherwise, the process returns to Stage 1.

C. Stage 3: AC–DC Network Integration

In Stage 3, the optional AC–DC network integration, the process steps are analogous to those of Stage 2. The interface is to be implemented according to the architecture presented in Fig. 17.

The control scheme for this stage must ensure that no stability-compromising behavior is exhibited in any parts of the entire system created by the AC–DC network integration. This system includes the DC network connected to the DC side of the AC grid interface and the AC network connected to the AC side of the AC grid interface. Also, the grid code of the AC grid has to be followed. Laboratory validation confirms stability before deployment.

With regard to safety, double or reinforced insulation must be used. Further, all provisions according to Table III have to be undertaken.

As discussed for Stage 2, the firmware of the SBBs in the swarm microgrid can be updated remotely. In contrast to installation works undertaken in previous stages, the installation of the AC grid interface must be done by a trained electrician.

While this Stage 3 is optional, it also presents a unique opportunity for enhancing sustainability beyond the location of the swarm microgrid by exporting electricity generated from renewable sources into an AC grid. The process then returns to Stage 1.

VI. Validation by Field Implementation and Laboratory Experimentation

In this section, real-world evidence of the practicality of the proposed methodology is presented, assessing the implementation of swarm microgrids in Bangladesh. These microgrids have been implemented following the "Quint-S" methodology process defined in Section V, in accordance with the design features presented in Section III and the design foundations of Section IV. With the support of the United Nations and other organizations, over 100 installations have been made [8], [44].

The DC swarm microgrid installation sites are located throughout the country. Many of these installations originate from marketplaces. Typical examples that reflect the three "S" design features are shown in Fig. 5. Self-serviceability on-site is also supported by a remotely located organization, relying on the ICT infrastructure to provide remote services. To this end, the communication tower shown in Fig. 5(a) provides swarm units with an access point for a wireless local area communication network and a gateway to connect to remote ICT facilities. Adaptations to a swarm microgrid being made on the roof of a warehouse are shown in Fig. 5(b), demonstrating self-serviceability regarding extension of power capabilities. In Fig. 5(c), several shops with roof-mounted solar panels are shown, illustrating sustainability by usage of 100% renewable energy. Fig. 5(d) stands for scalability: Using a donkey cart, additional swarm microgrid components are transported to a site for modular expansion of the swarm microgrid.

The following validation by field implementation makes use of remote monitoring data from installed swarm microgrids. The capability for remote monitoring is enabled by the deployed ICT infrastructure. The ICT infrastructure is implemented following the architecture design presented in Section III-A2. Details on particular realization aspects are shown in Fig. 6 and described as follows.

The ICT infrastructure relies on LANs using Wi-Fi technology. Key advantages of Wi-Fi technology are its wide availability and low cost. A disadvantage of Wi-Fi technology is the comparatively low range. This disadvantage can be overcome using repeaters, as shown in Fig. 6. A communication tower hosts a mobile telecommunication network gateway and a wireless LAN router to establish a wireless LAN, Wireless LAN-1. If the range of this Wireless LAN-1 is insufficient, a Wireless LAN Repeater-1 is used to establish a second LAN, Wireless LAN-2. All communication devices are powered from a swarm unit in their proximity, the respective user is compensated for the energy usage. For temporary situations, such as during installation and

(a) (b) (c) (d)

Fig. 5. Examples of practical realizations of the three design features as observed in various swarm microgrids in Bangladesh. (a) Self-serviceability: Communication tower containing a wireless local area network router. (b) Self-serviceability: Adaptations being made to a swarm microgrid in operation. (c) Sustainability: Several shops with solar panels, illustrating the usage of 100% renewable energy. (d) Scalability: Additional components being brought to a site for modular expansion of the swarm microgrid.

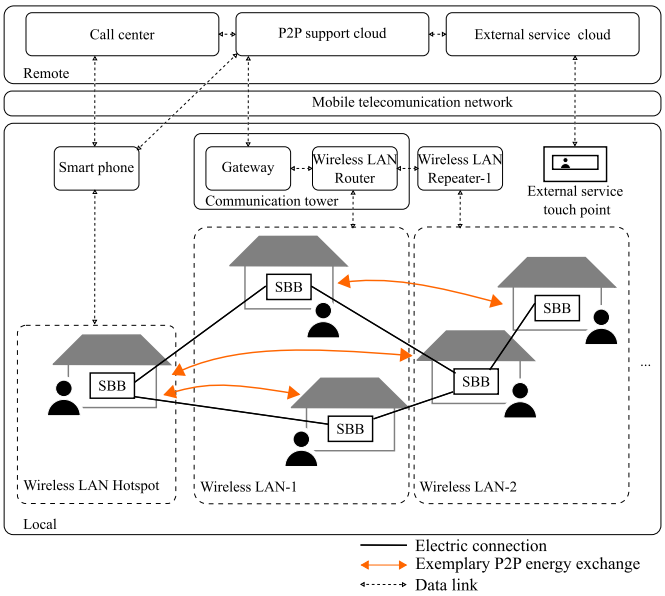

Fig. 6. Practical realization of the ICT infrastructure.

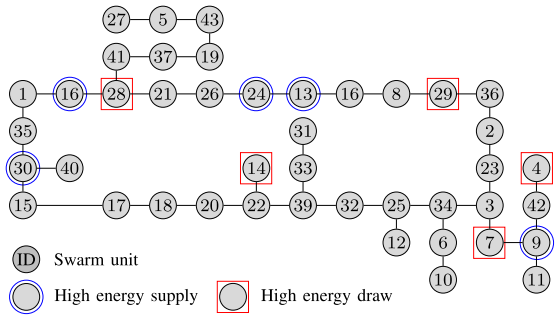

Fig. 7. Topology overview of a swarm microgrid installation.

troubleshooting, a smartphone can also establish a wireless LAN hotspot, as illustrated on the left side of Fig. 6.

P2P energy exchanges are not restricted to the SBBs within one wireless LAN. Instead, all swarm units of one swarm microgrid can engage in P2P energy exchange. For clarification, exemplary P2P energy exchanges between SBBs connected to different LANs but within the same swarm microgrid are illustrated in Fig. 6. The ICT infrastructure also includes external services, for example to facilitate prepaid balance top-up and cash-out through local service points. In addition, the call center may reach users on their phones to assist with troubleshooting.

The following subsections discuss the detailed validation, covering: 1) DC swarm microgrids in normal operation by assessing a specific swarm microgrid case study; and 2) DC swarm microgrids under contingency by assessing fault case scenarios in a laboratory environment.

A. *DC Swarm Microgrid in Normal Operation*

In this section, a practical example of a swarm microgrid deployment in Stage 1 as described in Table I and realized following the process of Fig. 4 is discussed. First, an overview of the site and the dataset is provided. Subsequently, the real-world implementations of the five "S" governing principles developed in this article are discussed.

1) Overview: This validation consists of the analysis of one particular real-world swarm microgrid over one month. The installation is located at a marketplace in northern Bangladesh on a so-called "chor," a river island. The assessment period is the month of September 2021. In Fig. 7, the ring-like topology with 43 swarm units and 43 cables is shown. The cable lengths, which are not represented to scale, range between 1 m and 30 m. The swarm microgrid voltage implemented is 12 V nominal, and no DC–DC converters are used in the SBBs of the deployed swarm units.

The users are mainly small business owners that operate at the market site. The market site has seen an early adoption of SHSs. The oldest system still in use was installed in the year 2000. Details of the individual SHS resources installed are provided in Table IV. For each swarm unit, the swarm unit identifier (ID), the installed solar PV generation capacity, the installed battery storage capacity, and the total load per swarm unit are provided. For each unit, additional data regarding the energy exchange performance for September 2021, such as the amount of energy drawn from the swarm microgrid, are provided.

The solar power generation capacity varies between 20 W and 480 W per swarm unit; some swarm units do not have any generation capacity. The battery capacity varies between 360 Wh and 5640 Wh; some units do not have any storage capacity. Still, the average storage capacity across all 43 swarm units is

TABLE IV
SWARM UNITS OF THE CASE STUDY SWARM MICROGRID: INSTALLED GENERATION AND STORAGE CAPACITY, CONNECTED LOAD, AND ENERGY EXCHANGE PERFORMANCE IN SEPTEMBER 2021

ID	Solar PV generation capacity [W]	Battery storage capacity [Wh]	Total load [W]	Energy drawn from network [Wh]	Proportion of total energy supplied [%]	Proportion of total energy drawn [%]
1	0	0	16	0	–	–
2	0	0	18	0	–	–
3	0	0	8	0	–	–
4	0	0	15	3 744	–	**6**
5	150	1 200	0	0	3	–
6	85	960	0	0	4	–
7	130	1 620	90	3 837	–	**7**
8	268	2 280	120	0	<1	–
9	50	720	0	4	**14**	<1
10	0	0	21	3 561	–	6
11	0	0	21	498	–	<1
12	50	660	25	775	–	1
13	268	2 520	160	0	**10**	–
14	250	1 560	130	12 219	–	**21**
15	0	0	48	2 660	–	5
16	85	1200	0	0	**20**	–
17	20	960	21	103	–	<1
18	0	0	10	2 218	–	4
19	250	2 280	140	2 853	–	5
20	250	2 280	150	0	<1	–
21	0	0	11	337	–	<1
22	85	960	0	0	7	–
23	85	960	0	0	3	–
24	100	1 200	0	0	**10**	–
25	20	360	15	1 263	–	2
26	0	0	11	2 322	–	4
27	0	0	8	0	–	–
28	250	1 560	160	7 894	–	**13**
29	60	780	78	5 163	–	**9**
30	85	1 200	0	0	**11**	–
31	480	5 640	180	119	–	<1
32	300	1 560	180	2 608	–	4
33	300	1 560	0	0	10	–
34	250	1 560	140	437	–	<1
35	0	0	10	1 389	–	2
36	85	960	0	1	6	<1
37	100	1 200	0	0	1	–
38	0	0	28	1 009	–	2
39	0	0	15	249	–	<1
40	480	5 640	275	2 191	–	4
41	240	2 280	140	900	–	2
42	0	0	23	0	<1	–
43	375	4 680	150	155	–	<1

1171 Wh per swarm unit. The total connected load per swarm unit varies between 8 W and 275 W, and some units do not have any connected load but instead specialize in selling energy to others.

Most swarm units actively pursued in peer-to-peer energy exchange. In the assessment period, 15 swarm units participated in peer-to-peer exchange by supplying energy, and 26 swarm units participated in peer-to-peer exchange by drawing energy. The amount of energy drawn per swarm unit in the assessed month ranges between 1 Wh and 12 kWh. A monthly energy draw of 12 kWh translates to a daily average of 402 Wh, which is below the energy exchange potential of 627 Wh described in Table II. Most units drew less than the reference value of 200 Wh per day defined as the KPR for Stage 1 in Table I. Moreover, some units did not draw any power at all. This may be due to a preference to only feed power into the network, or the fact that the corresponding loads may not have been in use during the assessment period.

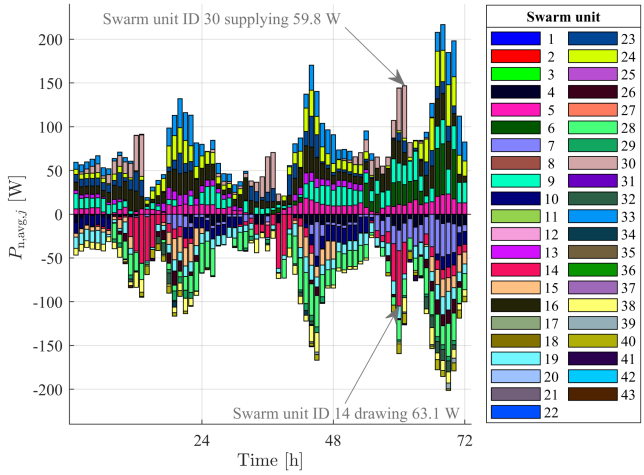

Fig. 8. Hourly average nodal power $P_{\mathrm{n,avg},j}$ of all swarm units j for the 72-h time period from September 28 to September 30, 2021.

Because the site is in a remote location with intermittent data connectivity, not all data points could be collected for all units. For the following energy exchange analysis, data points are aggregated to hourly averages. For every swarm unit, a total of 720 hourly averages are expected for the assessment period of 30 days. On average, 72% of these data are available.

A detailed example of the available data is shown in Fig. 8, covering a 3 day time frame from September 28, 2021 to September 30, 2021. The figure shows a stacked graph with all values of $P_{\mathrm{n,avg},j}$, the hourly average of the nodal power of each swarm unit j. As indicated in Fig. 2, positive values of $P_{\mathrm{n,avg},j}$ represent power supplied to other swarm units; negative values represent power drawn from other swarm units. In Fig. 8, the hourly average of the total power supplied by all swarm units corresponds to the positive stack, and the hourly average of the total power drawn by all swarm units corresponds to the negative stack. Except for some instances with missing data points, the waveforms of the total power drawn and the total power supplied are very similar in shape and magnitude. The largest power draw occurs in the evenings, in the last quarter of each 24 h interval. In the 72-h time period shown in Fig. 8, a total of 6.0 kWh were supplied to the network, whereas 5.6 kWh were drawn from the network, indicating a distribution loss of 7%.

The highest individual power throughput in Fig. 8 was achieved by swarm unit ID 14 in hour 60 when drawing an hourly average of 63.1 W. The highest power supply was achieved by swarm unit ID 30 in hour 61 when supplying an hourly average of 59.8 W. It is critical that power supply occurs at minimal SBB internal losses. Of concern are losses in the power electronic circuity in the SBB, as shown in Fig. 2. To this end, the hourly average power losses in the power electronic circuit, $P_{\mathrm{loss,PE,avg},j}$, for all SBBs supplying power in the assessed 72-h time period are provided in Fig. 9. The analysis shows that the power losses are small, with $P_{\mathrm{loss,PE,avg},j} < 2.1$W in the

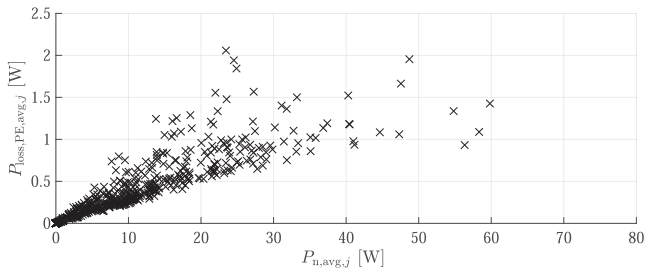

Fig. 9. Power losses of power electronic circuitry versus nodal power, operational data from September 28 to September 30, 2021.

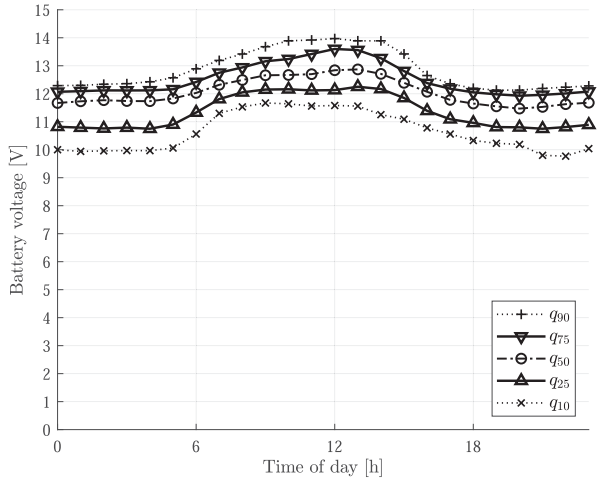

Fig. 10. Distribution of the battery voltages of all swarm units with battery storage for the month of September 2021, aggregated by hour of the day.

power range $P_{\mathrm{n,avg},j} < 60$ W. Still, these losses could be further reduced. Improvement options are discussed in Appendix D.

The remainder of this section analyzes the microgrid performance over the entire month of September 2021. The analysis is structured along the five "S" governing principles developed in this article. Accordingly, the three design features and then the two design foundations are discussed.

2) Self-Serviceability, Sustainability, and Scalability: Self-serviceability was ensured by deploying a technology that can be easily used and adapted. For assessing the ease of adaptation, the installation and modification record is reviewed. The swarm microgrid installation was initiated in March 2019. By the end of 2021, a total of 63 additions and modifications to the topology had been undertaken. Of these, 50% were implemented in the first year of operation, 46% in the second year, and 4% in the third year. Changes were made to the microgrid while the microgrid was in operation, demonstrating a high ease of adaptation.

As a second aspect relating to self-serviceability, the ease of use is examined. This is done by determining whether the technology can satisfy users' preferences with respect to energy exchange. These preferences are assessed by analyzing each swarm unit's energy exchange performance. In particular, the proportion of each swarm unit to total energy supply and to total energy draw are examined. These data are provided in the sixth and seventh columns of Table IV. The top five swarm units in terms of energy supply and energy draw are marked in Fig. 7 and highlighted in bold font in Table IV. In terms of the energy supplied, the top five swarm units contributed a total of 66% of all supplied energy. In terms of the energy drawn, the situation is more heterogeneous. The top five swarm units accounted for only 54% of the energy drawn from the network. Four units, ID1, ID2, ID3, and ID27, did not participate in the energy exchange during the assessed period. Only two units, ID9 and ID36, both supplied and drew energy during the assessment period. The remaining 37 of the 43 total units showed clear preferences for either only supplying or only drawing energy. The ease of use of the deployed technology allowed for the users to realize these clear preferences.

Sustainability is addressed by using only solar PV generation. When relying on such intermittent power generation technology, an important measure for ensuring a reliable supply is the availability of energy storage capacity. Therefore, the battery voltages for all swarm units that include batteries are assessed as follows. The deployed batteries use lead–acid chemistry. For this chemistry, the healthy battery voltage range is between 10.5 V and 14.5 V [42]. This analysis focuses on validating that the battery voltages remained in this range during the assessment period. This assessment was performed through statistical analysis of the battery voltage data using percentiles.

For the following percentile-based analyses, all available data points of the assessment time period are analyzed using a set of five specific parameters: The 10th percentile, q_{10}, and the 90th percentile, q_{90}, are used as indicators for the value range of the data points; the 25th percentile, q_{25}, and the 75th percentile, q_{75}, describe the interquartile range representing 50% of the data points; and finally, the 50th percentile q_{50}, which is the median.

The statistical analysis of the battery voltages for all swarm units with battery storage capacity are shown in Fig. 10, aggregated by hour of day. The waveforms reflect the solar-characteristic charging peak in the middle of the day and a prominent discharging pattern in the evening hours. The median values, indicated by q_{50}, are close to the nominal battery voltage of 12 V. The majority of the data, as indicated by the range between q_{25} and q_{75}, falls within the healthy battery voltage range. In addition, the 90th percentiles q_{90} also fall within the healthy range. However, the 10th percentiles q_{10} fall below the lower end of the healthy battery range during night hours. This can be explained by the fact that some of the batteries are very old and have been in operation for over 20 years. Still, the 10th percentiles q_{10} remain within the healthy range during the middle of the day, indicating a good battery maintenance charge.

Scalability is achieved by deploying a technology that allows for straightforward expansion. As discussed at the beginning of this section, multiple additions and reconfigurations have been made to the swarm microgrid. A key parameter for assessing successful scalability is consistency in the quality of service provided across all swarm units. In particular, the swarm node voltages should be close to the 1.0 p.u. level. For swarm unit j, the swarm node voltage $v_{\mathrm{n},j}$ is the voltage between the negative

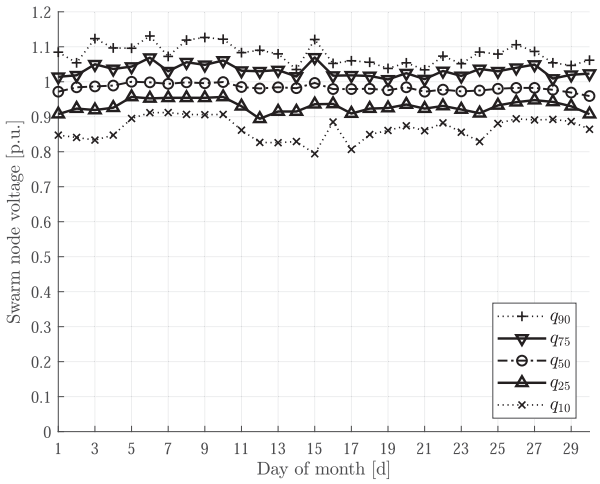

Fig. 11. Distribution of swarm node voltages for the month of September 2021, aggregated by day of the month.

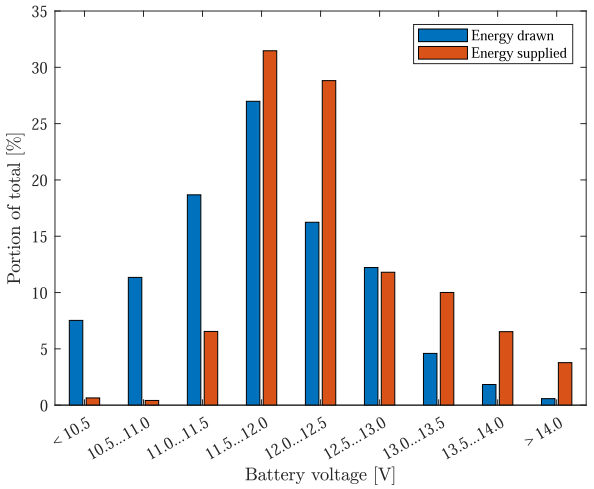

Fig. 12. Distribution of energy exchange quantities over battery voltage at the time of exchange.

and positive rails at the swarm node shown in Fig. 2. Swarm node voltages should be within a 1.0±0.2 p.u. range. This range definition relates to the healthy battery voltage range defined above and discussed for Fig. 10. The distribution of the swarm node voltages for all swarm units aggregated by day of month is shown in Fig. 11. The daily median values are very close to 1.0 p.u. Furthermore, the majority of all swarm node voltages fall within the 1.0±0.1 p.u. range. In addition, the values rarely extend outside the 1.0±0.2 p.u. range. Overall, the analysis shows a consistent service delivery across the swarm microgrid.

3) Stability and Safety: Stability is ensured by deploying a technology that is robust across a wide operating envelope. This wide operating envelope is defined by the large variations in the battery voltages of the swarm units. Therefore, it is important to verify that both power supply and power draw are possible across a wide range of battery voltages. To this end, Fig. 12 presents an assessment of the correlations between energy exchange and the battery voltage at which the energy exchange took place.

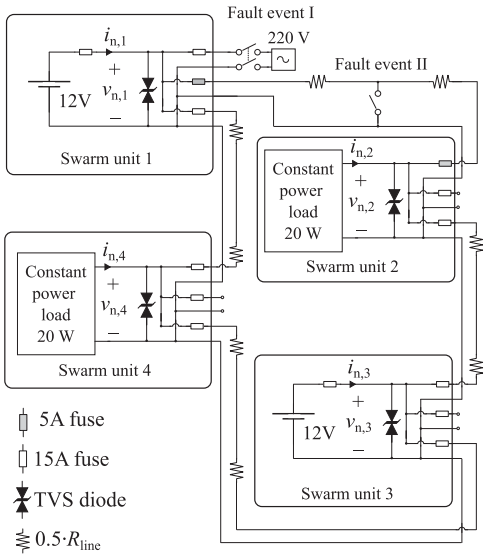

Fig. 13. Circuitry for laboratory contingency testing of DC swarm microgrid with $R_{\text{line}} = 0.2\ \Omega$.

Only swarm units with battery storage capacity, as indicated in Table IV, are included in this assessment. In terms of energy supplied, considerable contributions were made at battery voltages of 11.0 V and above; most of the energy supplied was transferred from swarm units with battery voltages above 12.0 V. In terms of energy drawn, a wider range of battery voltages can be observed. Still, most of the energy drawn by the swarm units was transferred at battery voltages below 12.0 V. In summary, as these data from September 2021 show, energy exchange is possible across a wide range of battery voltages. Thus, stability issues were not detected in practice. This observation is consistent with the results of a scientific investigation that showed swarm microgrids to be stable for up to at least 1000 participating swarm units [3].

The final design objective, safety, was addressed by implementing the safety measures detailed in Section IV. No safety-compromising incidents have been reported. A more indepth analysis of safety is presented in the following section.

B. DC Swarm Microgrid Under Contingency

An experimental validation in a laboratory environment was undertaken for two key contingency cases. The first case is an overvoltage event at a swarm unit, denoted as fault event I. The second case is a short circuit on a line, denoted as fault event II.

The circuitry used for the contingency testing is shown in Fig. 13. Details on the laboratory equipment used are provided in Appendix C. The reader is reminded of the internal structure of an SBB as indicated in Fig. 2. The system setup consists of four swarm units. Swarm units 1 and 3 act as suppliers, and swarm units 2 and 4 act as loads. Each swarm unit is equipped with industrial electronics in the form of a transient voltage suppression (TVS) diode at the swarm node. In addition, each cable port includes a fuse. The fuse tripping ratings are chosen as indicated in Fig. 13 to demonstrate the highest degree of

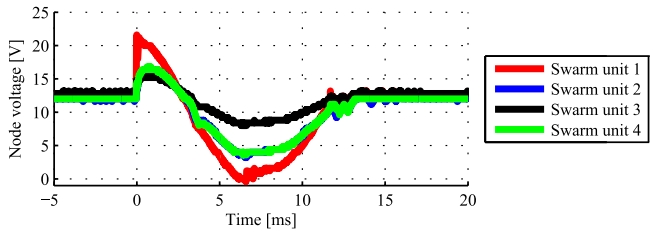

Fig. 14. Swarm unit's node voltages in laboratory contingency testing for fault event I, an overvoltage event at swarm unit 1.

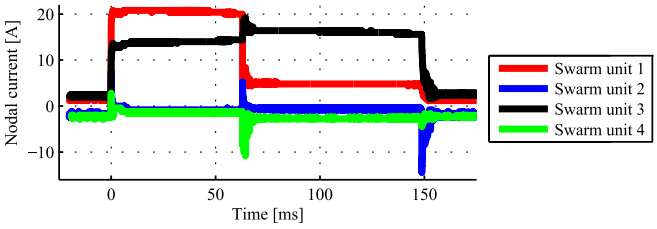

Fig. 15. Swarm units' nodal currents in laboratory contingency testing for fault event II, a short on the line between swarm units 1 and 2.

selectivity of zonal protection, with isolation of only the faulty branch while maintaining supply to all load points. Fault event I, an overvoltage on a node, is induced by connecting an AC supply to one of the cable ports of swarm unit 1. Fault event II, an overcurrent on a line, is induced by a short circuit on the line between swarm units 1 and 2.

The results for fault event I are provided in Fig. 14. After the contact to the AC supply is closed, the voltage at swarm unit 1 rises quickly. This has a system-wide effect of voltage increase. However, because of the TVS diode, this increase remains safely within the SELV range. The fuse of the cable port located between the TVS diode and the AC source, c.f. Fig. 13, disconnects the supply at $t = 7$ ms. After approximately 15 ms, the swarm microgrid has fully recovered.

The results for fault event II, a short circuit on the line between swarm unit 1 and swarm unit 2, are given in Fig. 15. After introducing the short circuit on the line, the nodal currents of both supplying nodes rise quickly, while swarm units 2 and 4 no longer receive sufficient power. The cable port fuse of swarm unit 1 trips after 65 ms. It takes another 90 ms for the cable port of swarm unit 2 to also trip, thus completing the zonal insulation of the fault. After less than 160 ms, the swarm microgrid has recovered and reached a new stable operating point.

VII. Conclusion

The novel "Quint-S" methodology for the technology design of peer-to-peer microgrids for swarm electrification was developed, implemented, and evaluated. The methodology is organized along a flowchart and follows the proposed three-plus-two set of "S" governing principles. The design is governed by the three "S" design features of sustainability, scalability, and self-serviceability, while respecting the two technical "S" foundations of safety and stability.

The first objective of sustainability is achieved by use of 100% renewable energy. The second objective of scalability is achieved through the design of a modular architecture in combination with a staged development plan. The designed swarm building blocks adopt the roles of seeds from which the growth within the first stage is stimulated. The modular design of the swarm building blocks readily allows for their interconnection as a low-voltage DC swarm microgrid, which is the result of the first development stage. The second stage builds on the first stage by connecting microgrids to a multi-microgrid system, as supported by the designed inter-microgrid interfaces. The third and final stage optionally connects the multi-microgrid system to the main AC grid, at a time when the two network systems reach geographic proximity. The third design objective of reaching self-serviceability is particularly important for the success of swarm electrification in remote areas. Professional technicians are required for installations only if a connection to AC grids is intended.

Safety and stability are the two technical foundations underlying the above design objectives. Stability is maintained, while safety relies on meeting standards of protection and further developing them according to the needs of swarm electrification. Dedicated laboratory experiments with overvoltage and short-circuit events confirmed the role of industrial electronics in meeting the safety expectations. The continuous operation of numerous field installations of the proposed microgrids further substantiates their ability to comply with the design foundations of safety and stability.

Laboratory validations and a real-world implementation case study confirmed that the combination of the principles of scalability, sustainability, self-serviceability, safety, and stability enables swarm electrification to serve as a practical, effective, and climate-friendly option for offering energy access with peer-to-peer energy exchange possibilities. Consequently, the comprehensive design methodology presented in this article offers a valuable contribution to the understanding and implementation of swarm microgrids.

Appendix

A) *Modular Architecture for Stage 2*

The integration of the IMI with the swarm microgrid is achieved by connecting the IMI to the battery of a swarm unit, as illustrated on the right side of Fig. 16. Bidirectional power flows are enabled by five sets of components inside the IMI, also shown in Fig. 16. First, a bidirectional meter records the energy traded between the two IMIs. Second, through a DC–DC conversion stage using step-up and step-down converters, the required power flows can be realized at flexible voltage bands. Third, a high-side switch and a low-side switch are required to select between the buying and selling paths. Fourth, the above components are connected to the DC link controller, which enables the automation of the IMI. Fifth, the power and control layer of the IMI is interfaced with its counterpart ICT layer. The IMI ICT entails a subset of the modules contained in the SBB ICT of Fig. 3. This subset comprises the user interface module, the data storage module, and the communication module that

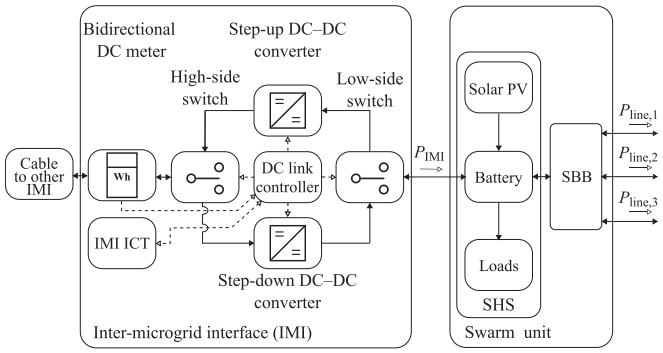

Fig. 16. Detailed modular architecture design for a DC swarm microgrid connection using inter-microgrid interfaces.

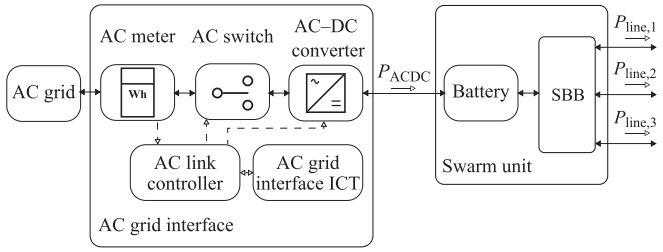

Fig. 17. Detailed modular architecture design for AC–DC network integration using an AC grid interface.

connects to the LAN. These three modules enable the remote monitoring and remote troubleshooting capabilities.

B) Modular Architecture for Stage 3

The integration of the AC grid interface with the swarm microgrid is achieved by connecting to the battery of a dedicated swarm unit without loads or solar PV, as shown in Fig. 17. This battery is used to buffer an intermittent supply from the AC grid. Power flows from the AC grid to the swarm microgrid are enabled by the following five components, as illustrated in Fig. 17. First, an AC meter provides the interface to the supply. Second, an AC switch allows for the controlled connection and disconnection of the AC grid from the swarm microgrid. Third, an AC–DC converter is used to achieve voltage and current conversion between the AC side and the DC swarm microgrid. Fourth, the above components are connected to the AC link controller, which allows for the automation of the AC grid interface. Fifth, the power and control layer of the AC grid interface is connected with its counterpart ICT layer. The AC grid interface ICT comprises the same modules as the IMI ICT, described above at the end of Appendix A.

C) Laboratory Equipment Details

For the experimental validation presented in Section VI-B, the following equipment was used. Lead–acid batteries were used to power swarm unit 1 and swarm unit 3. The constant power loads on swarm unit 2 and swarm unit 4 consisted of a boost converter with a constant voltage output supplying a 10-Ω resistor. Data collection was undertaken using 50-MHz scopes, model GDS-1054B. The short circuit for fault event II was produced by an electronic load, model PeakTech P2275, applying a 0.01-Ω fault path.

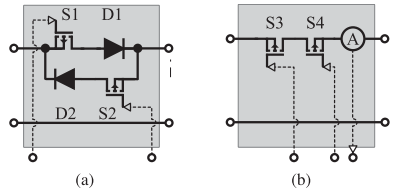

Fig. 18. Power electronic circuit alternatives to DC–DC converter in the SBB of Fig. 2: (a) MOSFET-diode circuit, (b) MOSFET-only topology.

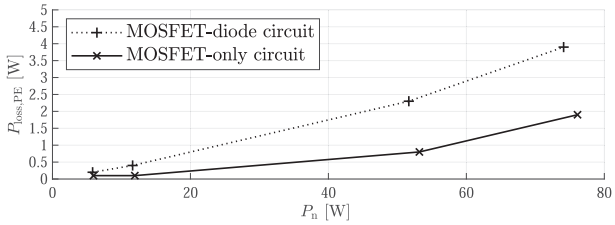

Fig. 19. Laboratory comparison of circuit alternatives, assessing power losses in the power electronic circuits at different levels of nodal power supply.

D) Alternative Power Electronic Circuits for SBBs

Alternative power electronic circuits may be used instead of a DC–DC converter in the SBB of Fig. 2. As discussed in Section III, such alternatives need to provide the capability to control the power flow direction based on control signals from the SBB controller of Fig. 2. Two circuits that can achieve this capability are discussed, as follows.

The MOSFET-diode circuit of Fig. 18(a) was used in the operational swarm microgrids assessed in Section VI. In this circuit, there are two antiparallel paths, each consisting of a controlled switch (S) and a diode (D). The MOSFET-only circuit is shown in Fig. 18(b). Here, the diodes are omitted. Instead, two back-to-back controlled switches are used. In this circuit, the current is monitored, and the switches are opened when the current flows in an undesired direction.

The power losses in the power electronic circuit $P_{\text{loss,PE}}$ for both topologies were compared in a laboratory environment using the following components. D1 and D2 were implemented as Schottky diodes with a typical forward voltage of 0.5 V. Switches S1–S4 were implemented using MOSFETs with a rated ON-state resistance of less than 5 mΩ.

The experimental results are shown in Fig. 19. Generally, the losses in the power electronic circuits are low, for low levels of nodal power supply P_{n}. For the MOSFET-diode circuit $P_{\text{loss,PE}} < 4\,\text{W}$, whereas for a MOSFET-only circuit $P_{\text{loss,PE}} < 2\,\text{W}$ for the assessed power range. Therefore, the MOSFET-only circuit represents an attractive alternative to the MOSFET-diode circuit.

ACKNOWLEDGMENT

The authors would like to thank the ME SOLshare operations and data teams who provided the raw data for the case study presented in this work, as well as the ME SOLshare laboratory team who provided the measurements presented in Appendix D.

REFERENCES

[1] IEA, IRENA, UNSD, WB, and WHO, "Tracking SDG 7: The energy progress report 2023," IEA, Paris, Tech. Rep. 6, 2023.

[2] S. Groh, D. Philipp, B. E. Lasch, and H. Kirchhoff, "Swarm electrification: Investigating a paradigm shift through the building of microgrids bottom-up," in *Proc. Decentralized Solutions Developing Economies: Addressing Energy Poverty Through Innov.*, (Series Springer Proceedings in Energy), S. Groh, J. V. Straeten, B. E. Lasch, D. Gershenson, W. L. Filho, and D. M. Kammen, Eds., Cham, Switzerland: Springer, 2015, pp. 3–22.

[3] H. Kirchhoff and K. Strunz, "Control and stability of modular DC swarm microgrids," *IEEE J. Emerg. Sel. Topics Power Electron.*, vol. 10, no. 5, pp. 6274–6292, Oct. 2022.

[4] K. Strunz, E. Abbasi, and D. N. Huu, "DC microgrid for wind and solar power integration," *IEEE J. Emerg. Sel. Topics Power Electron.*, vol. 2, no. 1, pp. 115–126, Mar. 2014.

[5] H. Arya and M. Das, "Fast charging station for electric vehicles based on DC microgrid," *IEEE J. Emerg. Sel. Topics Ind. Electron.*, vol. 4, no. 4, pp. 1204–1212, Oct. 2023.

[6] V. Vossos, D. Gerber, Y. Bennani, R. Brown, and C. Marnay, "Techno-economic analysis of DC power distribution in commercial buildings," *Appl. Energy*, vol. 230, pp. 663–678, 2018.

[7] G. Heinemann, "Innovating in the off-grid sector: Sustainable supply chains and business models for solar home system provision in Bangladesh and Kenya," *Energy Res. Social Sci.*, vol. 94, 2022, Art. no. 102853.

[8] P. Fairley, "'Swarm electrification' powers villages: ME SOLshare links isolated PV systems," *IEEE Spectr.*, vol. 55, no. 4, p. 21, Apr. 2018.

[9] ESMAP, "Beyond connections: Energy access redefined," World Bank, Washington D.C., USA, Tech. Rep. 008/15, Jun. 2015.

[10] F. F. Nerini, O. Broad, D. Mentis, M. Welsch, M. Bazilian, and M. Howells, "A cost comparison of technology approaches for improving access to electricity services," *Energy*, vol. 95, pp. 255–265, 2016.

[11] R. Dumitrescu, A. Lüth, J. Weibezahn, and S. Groh, "Prosumer empowerment through community power purchase agreements: A market design for swarm grids," *Energy J.*, vol. 11, no. 1, pp. 842–857, Jan. 2022.

[12] S. Sheridan, K. Sunderland, and J. Courtney, "Swarm electrification: A comprehensive literature review," *Renewable Sustain. Energy Rev.*, vol. 175, 2023, Art. no. 113157.

[13] F. S. Al-Ismail, "DC microgrid planning, operation, and control: A comprehensive review," *IEEE Access*, vol. 9, pp. 36154–36172, 2021.

[14] H. Louie, *Off-Grid Electrical Systems in Developing Countries*. Cham, Switzerland: Springer, 2018.

[15] H. Kirchhoff and K. Strunz, "Key drivers for successful development of peer-to-peer microgrids for swarm electrification," *Appl. Energy*, vol. 244, pp. 46–62, 2019.

[16] P. A. Madduri, J. Poon, J. Rosa, M. Podolsky, E. A. Brewer, and S. R. Sanders, "Scalable DC microgrids for rural electrification in emerging regions," *IEEE J. Emerg. Sel. Topics Power Electron.*, vol. 4, no. 4, pp. 1195–1205, Dec. 2016.

[17] IEC, "Specifications for SELV DC systems conforming to the ESMAP multi-tier framework tier 2 and tier 3 requirements for household electricity supply," Standard IEC 63318, 2022.

[18] M. Nasir, Z. Jin, H. A. Khan, N. A. Zaffar, J. C. Vasquez, and J. M. Guerrero, "A decentralized control architecture applied to DC nanogrid clusters for rural electrification in developing regions," *IEEE Trans. Power Electron.*, vol. 34, no. 2, pp. 1773–1785, Feb. 2019.

[19] A. Werth, N. Kitamura, and K. Tanaka, "Conceptual study for open energy systems: Distributed energy network using interconnected DC nanogrids," *IEEE Trans. Smart Grid*, vol. 6, no. 4, pp. 1621–1630, Jul. 2015.

[20] IEEE, "Standard for DC microgrids for rural and remote electricity access applications," Standard IEEE 2030.10," 2021.

[21] E. Bullich-Massagué, F. Díaz-González, M. Aragüés-Peñalba, F. Girbau-Llistuella, P. Olivella-Rosell, and A. Sumper, "Microgrid clustering architectures," *Appl. Energy*, vol. 212, pp. 340–361, 2018.

[22] Z. Zhao et al., "Energy transaction for multi-microgrids and internal microgrid based on blockchain," *IEEE Access*, vol. 8, pp. 144362–144372, 2020.

[23] S. Hirmer and H. Cruickshank, "The user-value of rural electrification: An analysis and adoption of existing models and theories," *Renewable Sustain. Energy Rev.*, vol. 34, pp. 145–154, 2014.

[24] A. Riccobono and E. Santi, "Comprehensive review of stability criteria for DC power distribution systems," *IEEE Trans. Ind. Appl.*, vol. 50, no. 5, pp. 3525–3535, Sep./Oct. 2014.

[25] E. Espina, J. Llanos, C. Burgos-Mellado, R. Cárdenas-Dobson, M. Martínez-Gómez, and D. Sáez, "Distributed control strategies for microgrids: An overview," *IEEE Access*, vol. 8, pp. 193412–193448, 2020.

[26] M. O. Godinho, W. C. Leal, R. F. Moreto, C. R. D. Aguiar, and R. Q. Machado, "SoC-Adaptive power sharing strategy applied to DC microgrids supplied by multiple energy storage systems," *IEEE J. Emerg. Sel. Topics Ind. Electron.*, vol. 4, no. 4, pp. 1224–1234, Oct. 2023.

[27] J. Liao, C. Guo, Y. Huang, G. Qiu, N. Zhou, and Q. Wang, "Active damping control of cascaded DC converter in DC microgrids based on optimized parallel virtual resistance," *IEEE J. Emerg. Sel. Topics Ind. Electron.*, vol. 4, no. 2, pp. 560–570, Apr. 2023.

[28] T. Dragicevic, X. Lu, J. Vasquez, and J. Guerrero, "DC microgrids—Part II: A review of power architectures, applications and standardization issues," *IEEE Trans. Power Electron.*, vol. 31, no. 5, pp. 3528–3549, May 2016.

[29] L. Mackay, E. Vandeventer, and L. Ramirez-Elizondo, "Circulating net currents in meshed DC distribution grids: A challenge for residual ground fault protection," *IEEE Trans. Power Del.*, vol. 33, no. 2, pp. 1018–1019, Apr. 2018.

[30] U. Orji et al., "Adaptive zonal protection for ring microgrids," *IEEE Trans. Smart Grid*, vol. 8, no. 4, pp. 1843–1851, Jul. 2017.

[31] J. J. Justo, F. Mwasilu, J. Lee, and J.-W. Jung, "AC-microgrids versus DC-microgrids with distributed energy resources: A review," *Renewable Sustain. Energy Rev.*, vol. 24, pp. 387–405, Aug. 2013.

[32] D. Kumar, F. Zare, and A. Ghosh, "DC microgrid technology: System architectures, AC grid interfaces, grounding schemes, power quality, communication networks, applications, and standardizations aspects," *IEEE Access*, vol. 5, pp. 12230–12256, 2017.

[33] G. Prevedello and A. Werth, "The benefits of sharing in off-grid microgrids: A case study in the Philippines," *Appl. Energy*, vol. 303, Dec. 2021, Art. no. 117605.

[34] M. A. G. Mitolo, *Electrical Safety of Low-Voltage Systems*. New York, NY, USA: McGraw-Hill, 2009.

[35] P. E. Sutherland, *Principles of Electrical Safety*. Hoboken, NJ, USA: Wiley, 2015.

[36] S. Dutta and K. Chatterjee, "An AC-DC hybrid nanogrid system for PV and battery storage based futuristic buildings," *IEEE J. Emerg. Sel. Topics Ind. Electron.*, vol. 2, no. 3, pp. 314–323, Jul. 2021.

[37] B. Soltowski, F. Stewart, S. Strachan, D. Campos-Gaona, O. Anaya-Lara, and S. Galloway, "A field trial of off-grid SHS interconnection in Rwanda's northern province," *Energy Sustain. Develop.*, vol. 66, pp. 69–78, 2022.

[38] F. Xue, R. Yu, and A. Q. Huang, "A 98.3% efficient GaN isolated bidirectional DC converter for DC microgrid energy storage system applications," *IEEE Trans. Ind. Electron.*, vol. 64, no. 11, pp. 9094–9103, Nov. 2017.

[39] T. S. Ustun, S. M. S. Hussain, H. Kirchhoff, B. Ghaddar, K. Strunz, and I. Lestas, "Data standardization for smart infrastructure in first-access electricity systems," *Proc. IEEE*, vol. 107, no. 9, pp. 1790–1802, Sep. 2019.

[40] T. Gönen, *Electric Power Distribution Engineering*, 3rd ed., Boca Raton: Taylor and Francis, 2014.

[41] A. Nourai, V. I. Kogan, and C. M. Schafer, "Load leveling reduces T&D line losses," *IEEE Trans. Power Del.*, vol. 23, no. 4, pp. 2168–2173, Oct. 2008.

[42] M. Hankins, *Stand-Alone Solar Electric Systems: The Earthscan Expert Handbook for Planning, Design, and Installation*. Sterling, VA, USA: Earthscan, 2010.

[43] M. Hamzeh, M. Ghafouri, H. Karimi, K. Sheshyekani, and J. M. Guerrero, "Power oscillations damping in DC microgrids," *IEEE Trans. Energy Convers.*, vol. 31, no. 3, pp. 970–980, Sep. 2016.

[44] UNDESA, "UN awards US $1 million for Bangladesh solar entrepreneurship initiative to aid rural electrification," Nov. 2017. [Online]. Available: https://www.un.org/

Hannes Kirchhoff received the M.Sc. degree in renewable energy systems, in 2013, from TU Berlin, Berlin, Germany, where he received the Dr.-Ing. degree from the Chair of Sustainable Electric Networks and Sources of Energy (SENSE) in 2023.

He was a Technical Consultant with MicroEnergy International on several projects in Asia and Africa undertaking technology, supplier, and value chain assessments. As a Cofounder, Chief Technology Officer, and Senior Technical Advisor with ME SOLshare, he has been contributing to the pioneering frontier of innovative energy access solutions using DC microgrid technologies since 2015.

Kai Strunz received the Dr.-Ing. degree (*summa cum laude*) from Saarland University, Saarbrücken, Germany, in 2001.

From 1995 to 1997, he was with Brunel University, London, U.K.. From 1997 to 2002, he was with the Division Recherche et Dévelopment of Electricité de France, Paris, France. From 2002 to 2007, he was Assistant Professor of electrical engineering with the University of Washington, Seattle, USA. Since 2007, he has been a Professor of sustainable electric networks and sources of energy with TU Berlin, Berlin Germany, and since 2017, he has been a Guest Professor with the Chinese Academy of Sciences, Beijing, China.

Dr. Strunz was the recipient of the IEEE PES Prize Paper Award in 2015 and 2023, the *Journal of Emerging and Selected Topics in Power Electronics* First Prize Paper Award 2015, and the 2020 Best Paper Award in the field of electric machines and drives by IEEE TRANSACTIONS ON ENERGY CONVERSION. He was the Chairman of the Conference IEEE PES Innovative Smart Grid Technologies Europe in 2012. He is the chair of the IEEE PES Subcommittee "Distributed Energy Resources" and the co-chair of the IEEE Working Group "Dynamic Performance and Modeling of HVDC Systems and Power Electronics for Transmission Systems". On behalf of the Intergovernmental Panel on Climate Change (IPCC), he acted as the Review Editor for the Special Report on Renewable Energy Sources and Climate Change Mitigation.